

Glass Transition as a Key to Identifying Solid Phases

Bernhard Wunderlich^{1,2}

¹Department of Chemistry, University of Tennessee, Knoxville, Tennessee 37996-1600

²Chemical Sciences Division, Oak Ridge National Lab, Oak Ridge, Tennessee 37831-6197

Received 26 February 2006; accepted 12 May 2006

DOI 10.1002/app.26110

Published online in Wiley InterScience (www.interscience.wiley.com).

ABSTRACT: The earlier suggested definition, “a solid is a condensed phase at a temperature below its glass transition,” has developed into the key to the understanding of macromolecular materials. Its importance and implications for the understanding of not only polymers but all materials are reviewed in this article. A macromolecular sample can be a system consisting of a single amorphous phase or be a molecularly coupled multiphase system of different degrees of order and metastability in its subsystems. It is well known that liquid crystals, plastic crystals, and conformationally disordered crystals are still ordered above the glass transition, but recently even the monoclinic crystals of poly (oxyethylene) have been shown to have an additional glass transition below the melting temperature. This supports the inference that in the delineation of the solid state, the glass transitions take preference to melting transitions. The main tools for recognizing the different equilibrium and nonequilibrium phases are differential scanning calorimetry and tem-

perature-modulated differential scanning calorimetry. Such calorimetry yields quantitative heat capacities to be interpreted in terms of molecular motion and latent heats. Separated into reversible and irreversible contributions, the entropy changes connected to ordering and disordering can be evaluated. The value of the recognition of phase transitions lies in the fact that materials must be pliable for being manufactured into a final shape but often need high modulus and strength in their applications. Near the glass transition, forming is easy, whereas below the glass-transition temperature, a high modulus is reached for properly oriented polymer molecules. By the identification of the glass transitions of materials with different states of order, a better understanding of the solid state of soft materials is reached. © 2007 Wiley Periodicals, Inc. *J Appl Polym Sci 105: 49–59, 2007

Key words: calorimetry; crystallization; glass transition; thermal properties

INTRODUCTION

Macroscopic and microscopic description of materials

The macroscopic picture of materials is based on a scale commensurate with the human senses. Its scientific base developed over the last 200 years on experimental knowledge, mainly gained from substances of simple, small molecules. The early quantitative experiments consisted of gravimetry, dilatometry, calorimetry, and mechanical analyses, the core techniques of thermal analysis.¹ The first major theoretical tool was equilibrium thermodynamics, which reached its final form and central place in applications early in the 20th century. By now, its link to the thermodynamics of ir-

reversible processes is also well established² and will be of importance in this review of the interplay between the glass transition, melting transition, and solidity of ordered materials.

With the increasing understanding of macromolecules during the 20th century, the systems of interest were increasingly removed from equilibrium, and thermodynamics fell into disuse in favor of concentrating on the newly emerging microscopic understanding of molecular structure and motion. Although the microscopic structural model of materials could easily be bridged to their macroscopic appearance, the link of the microscopic molecular motion to the thermal properties caused difficulties, particularly in the field of macromolecules. Although the structure model involves a factor of 10^3 in the translation of the molecular sizes in the nanometer scale to the lower limit of the macroscopically recognizable micrometer, a factor of 10^9 is needed to go from the timescale of atomic motion in picosecond or faster ranges to the humanly recognizable milliseconds. To understand the macroscopic thermal and mechanical response of a material is thus much more difficult, and the realization of the connection is the goal of 21st century thermal analysis.³ To fully judge a material, it is necessary to know both the structure and thermal properties, as illustrated in this article.

This article is dedicated to the memory of Professor Marian Kryszewski.

This article has been authored by a contractor of the U.S. Government under contract number DOE-AC05-00OR22725. Accordingly, the U.S. Government retains a nonexclusive, royalty-free license to publish or reproduce the published form of this contribution, or allow others to do so, for U.S. Government purposes.

Correspondence to: B. Wunderlich (wunderlich@chartertn.net).

Journal of Applied Polymer Science, Vol. 105, 49–59 (2007)
© 2007 Wiley Periodicals, Inc. *This article is a US Government work and, as such, is in the public domain in the United States of America.

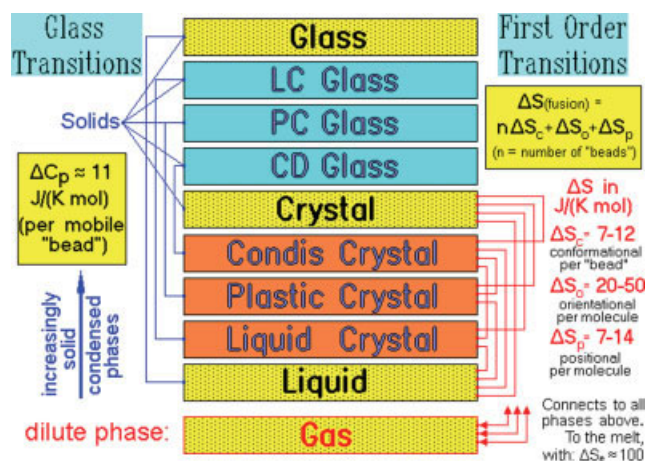


Figure 1 Schematic of the types of phases and possible transitions between the phases. The trends in the properties and the changes in the heat capacity at the glass transition and entropy contributions to the changes in the disorder are also listed. The shaded boxes represent the classical phases. [Color figure can be viewed in the online issue, which is available at www.interscience.wiley.com.]

Phase structure of polymeric materials

The common semicrystalline polymers have a multiphase structure with boundaries that are frequently crossed by the macromolecules. A phase, as commonly assumed, consists of a homogeneous, macroscopic volume of matter separated by well-defined surfaces of negligible influence on the overall phase properties.¹ Domains in a sample that differ in the composition or physical state are considered different phases. When the size of a macroscopic phase is decreased to a microphase, for example, in colloids, the surface becomes nonnegligible. Further decreases in the size to nanophases yields properties that are different from those of the bulk phase in many aspects.⁴ Finally, when atomic dimensions are reached, the phase concept has no value because of the loss of homogeneity.

In case a phase is not in equilibrium, the concepts of irreversible thermodynamics must be followed for the description of the sample.² In semicrystalline polymers, the different phases are to be considered subsystems of an overall system that is always far from equilibrium. The macromolecules are sufficiently long to participate in more than one of these subsystems and will decouple at the interface while still transferring stress to affect the properties of the adjacent phases.

A summary of possible phases was developed some 25 years ago.⁵ In its development, both the molecular structure and mobility were considered. A schematic representation is reproduced in Figure 1. The four classical phases are gas, liquid, crystal, and glass. The gas is the only dilute phase. Its structure and molecular motion are well described by the ideal gas law.¹ All other phases in Figure 1 are condensed phases,

with their molecules in direct contact and their motions variously restricted. Intermediate in order between the liquid and crystal are the mesophases, which retain some of the large-amplitude motion of the liquid. Liquid crystals (LCs) are positionally largely disordered, but they have a small amount of orientational order in one or two directions of space. Plastic crystals, in contrast, have full positional order, usually described by a cubic or hexagonal lattice, but are orientationally mobile; that is, their close-to-spherical molecules rotate. Conformationally disordered (condis) crystals display internal rotations about specific covalent bonds but are otherwise orientationally and positionally ordered.⁶ Note that all these mesophases show large-amplitude motion in addition to the always present small-amplitude, vibrational motion.

Typical thermodynamic parameters describing the differences between the phases are listed in Figure 1 near the lines indicating the glass and first-order transitions. The values are derived from the Advance Thermal Analysis System (ATHAS) Data Bank.⁷ For polymers, the conformational disorder is most prominent. The number of mobile units (n), also called the number of mobile beads, allows estimates of both the change in the heat capacity at the glass transition and the entropy of disordering on melting. It is shown in this article that the change in the heat capacity during first-order transitions is the macroscopic indicator of the change in the large-amplitude motion and plays a major role in understanding the mechanical properties and the proper interpretation of thermal analyses.

Link of the heat capacity to the molecular motion and thermodynamic functions

The three integral thermodynamic functions are the enthalpy (H), entropy (S), and free enthalpy (G), and they are evaluated from calorimetric measurements of the heat capacity (C_p) and latent heat. At a low temperature, adiabatic calorimetry is used, and at higher temperatures, differential scanning calorimetry (DSC) is used. The latent heats, which for polymers often cannot be measured under equilibrium conditions, must be separated from the thermal effects due to the heat capacity for evaluation (baseline method).¹ Finally, modulated-temperature differential scanning calorimetry (TMDSC) has been developed over the last 15 years. It involves the superposition of a small, periodic temperature change on the temperature profile of the measurement. By the deconvolution of the total and reversing responses to the modulation, it is possible to evaluate the reversibility of the system and to compute irreversible processes and reversible changes within the phase structures.¹ With TMDSC, a direct measurement is possible to identify arrested equilibria, which are common in linear macromolecules.⁸

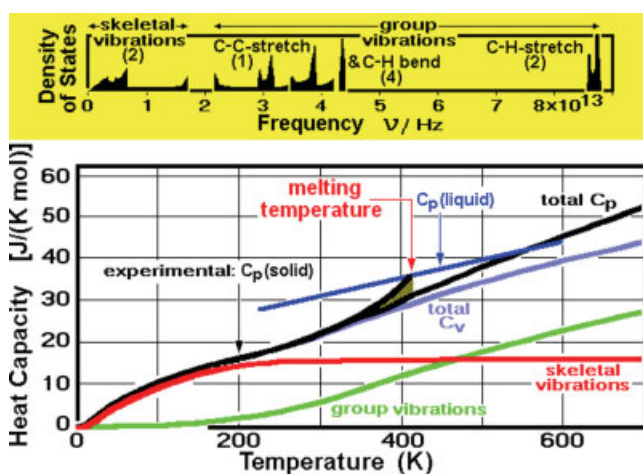


Figure 2 Experimental and calculated heat capacity contributions for polyethylene. The upper curve shows a plot of the vibrational densities of state.⁹ The equilibrium melting temperature is 414.6 K, and the entropy of fusion is $10.5 \text{ J K}^{-1} \text{ mol}^{-1}$.⁷ [Color figure can be viewed in the online issue, which is available at www.interscience.wiley.com.]

The link of the experimental heat capacity of polyethylene to an appropriate vibrational spectrum from a normal mode analysis⁹ is illustrated in Figure 2. The low-temperature heat capacity is fitted to one- and three-dimensional Debye functions¹⁰ to model the skeletal vibrations.^{11,12} The result is an approximation of the lower group of frequencies, representing the intermolecular vibrations, and a group resulting mainly from the torsional and transverse backbone modes of vibration. The group vibrations at distinctly higher frequencies are then approximated by Einstein functions¹³ and box distributions.¹² The curve for the total C_p includes the conversion from the heat capacity at a constant volume to a constant pressure and represents the vibrational contribution to the heat capacity. It can be used as a baseline to observe the beginning large-amplitude motion, which consists in macromolecules mainly of conformational motion, whereas small molecules may exhibit mainly translational motion and rotations of the whole molecule. Note that C_p , and with it H , are rather insensitive to equilibrium. Above 50 K, the crystals and glass have close to the same heat capacity. Below 50 K, the glass has a higher heat capacity because of its lower acoustic vibration frequencies, but the absolute value of C_p in this temperature range is so low that H is little affected by this difference. The structure of the supercooled liquid gets arrested at the glass transition while changing to a solid. Microscopically, the large-amplitude motion stops, and its kinetic and potential energy contributions change to those of the corresponding vibrations. For polymers, these are the corresponding torsional vibrations. The external contribution to C_p , calculated from expansivity and compressibility, changes from the larger value of the liquid to the smaller one of the

solid. For polyethylene, all these quantities are sufficiently well known from the measurement of the thermal parameters and calculation of the molecular motion to evaluate even the equilibrium-related quantities S and G down to the absolute zero of temperature. This can be done not only for the equilibrium crystal but also for the glass and the supercooled liquid (assuming that for the supercooled liquid the arrest of equilibrium can be avoided to 0 K).¹⁴ The entropy of the crystals at 0 K is $0 \text{ J K}^{-1} \text{ mol}^{-1}$, set by the third law. The glass has an experimental value of $+2.59 \text{ J K}^{-1} \text{ mol}^{-1}$. The supercooled liquid is extrapolated to $+0.41 \text{ J K}^{-1} \text{ mol}^{-1}$. As expected, there is no indication of the Kauzmann paradox¹⁵ (an unreasonable negative entropy). The respective values for G are H_o^o , $H_o^o + 2.5 \text{ kJ/mol}$, and $H_o^o + 2.1 \text{ kJ/mol}$, where H_o^o is the enthalpy of the crystal at 0 K. For comparison, the heat of fusion is 4.11 kJ/mol at the equilibrium melting temperature of 414.6 K.

A more detailed view of the complete set of motions within a crystallized macromolecule can be obtained from molecular dynamics simulation by a supercomputer, as summarized in Figure 3.¹⁶ Besides the fast vibrational motion, represented by the displacements noticeable at A, B, and C, there is a slower defect generation in the form of gauche conformations within the crystals. The time interval presented in Figure 3 shows the change from a polyethylene chain placed in an ideal relationship to the crystal lattice at time zero through the random generation of the three modes of vibration by the addition of the proper amount of kinetic energy to reach 320 K. In the later stages, the figure represents the process of a phonon collision,

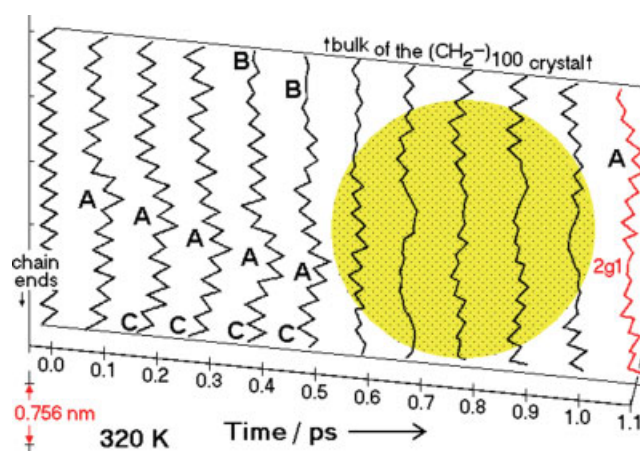


Figure 3 Supercomputer simulation of a chain end inside a polyethylene crystal as a function of time: (A) transverse vibration, (B) torsional vibration, and (C) longitudinal vibration. The collision of the three phonons is marked by the shaded area. The kink defect 2gt consists of a gauche-trans-gauche sequence and has an average lifetime of the order of magnitude of 1 ps.¹⁶ [Color figure can be viewed in the online issue, which is available at www.interscience.wiley.com.]

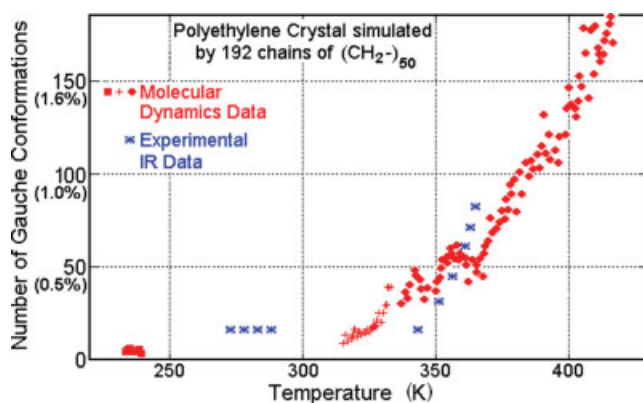


Figure 4 Experimental gauche concentrations in paraffins and concentrations calculated by supercomputer simulation, both as a function of the temperature, as presented earlier.^{16–18} [Color figure can be viewed in the online issue, which is available at www.interscience.wiley.com.]

which generates an isolated defect of higher potential energy, consisting of two gauche conformations and one trans conformation (2g1). This defect consists of a 180° rotation of the chain, as can be seen at the bottom of the drawing, in which the final bond points to the right instead of to the left as in the earlier stages of the modulation.

The average number of gauche conformations as a function of time is given in Figure 4. It is generated by simulations similar to those in Figure 3 and compared with experiments of infrared analyses with paraffins.^{16–18} In Figure 5, the heat capacity effect of such defects is demonstrated for the case of glassy and crystalline polyethylene. The large-amplitude motion in the defect formation and collapse is contained locally and in polyethylene does not cause a change into a phase of a different structure. The glass transition and melting transition, which require cooperative defect formation, occur at a distinctly higher temperature. The sequence of Figures 2–5 illustrates the link of the macroscopic C_p to its molecular motion, a link that also is at the root of the differences between the phases in Figure 1 and the definition of solids and liquids to be discussed.

DEFINITION OF SOLIDS AND LIQUIDS

Concentrating on the condensed phases in Figure 1, one can see that it is not easy to find a sharp delineation of liquid and solid phases. In fact, there has never been a satisfying scientific definition of the word *solid* based on structure alone. The dictionary definition of the noun *solid*¹⁹ goes back to the 15th century, and its modern wording is as follows: “a substance that does not flow perceptibly under moderate stress, has a definite capacity for resisting forces (as compression or tension) which tend to deform it, and under ordinary

conditions retains a definite size and shape.” This statement of common experience is not suitable as an operational definition of the type proposed by Bridgman.²⁰ In an operational definition, a precise operation (experiment) is to be specified to answer the question about the subject to be defined. In the dictionary definition, there are no quantitative limits given to make it scientifically acceptable for the terms: imperceptible flow, moderate stress, definite capacity for resistance, forces that tend to deform, and definite shape.

For a long time, it was assumed that only crystals are true solids. Even at present, glasses are sometimes called supercooled liquids, despite their easily proven hardness. In fact, there are a number of mechanical properties that have in the past been used to characterize the glass-transition temperature (T_g): at T_g , the viscosity of polymers commonly reaches about 10^{13} P (which equals 1 TPa s); the polymers reach the brittle point for fracture at T_g ; and above T_g , threads can be pulled from a viscous liquid (thread-pull temperature). Crystals at the melting temperature (T_m), in contrast, vary widely in their mechanical properties. Some crystals are much softer than glasses and flow on the application of lower stresses. Just consider perfluorocyclohexane, a perfect, face-centered cubic (FCC) crystal. It cannot hold its shape, but it flows.²¹ The trigonal polytetrafluoroethylene crystals increase in shear viscosity with temperature, and on disordering, given a high enough molar mass, the melt has an even higher shear viscosity.²² Checking the behavior of the condensed phases in Figure 1, we find that the solidity increases from liquid to mesophases to crystals, but a specific boundary cannot easily be identified with the degree of order. This also can be documented by the glasses of the mesophases, which are placed at the top of the diagram between the classical crystal and the classical (amorphous) glass. All mesophases become solid on vitrification without changing their structure.

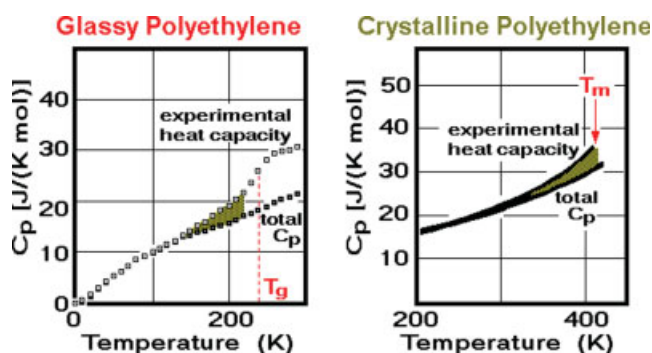
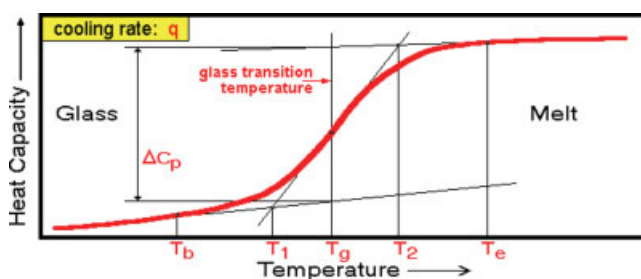


Figure 5 C_p contribution of gauche defects at temperatures below T_g and below T_m of the crystals (cf. Fig. 2).¹ [Color figure can be viewed in the online issue, which is available at www.interscience.wiley.com.]



The seven characteristic parameters of the glass transition

A solid is a condensed phase at a temperature below the glass transition.

Figure 6 Schematic of the glass transition analyzed on cooling and its defining parameters.¹ [Color figure can be viewed in the online issue, which is available at www.interscience.wiley.com.]

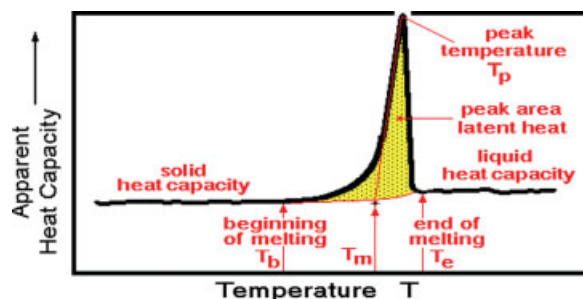
For glasses, there is little problem with using T_g as the operational definition to distinguish a solid from a liquid. Indeed, the mechanical properties change at T_g , from those of a hard and usually brittle solid to liquid-like properties, as pointed out previously. On cooling through the glass transition, the structure of the material does not change, but the cooperative, large-amplitude molecular motion stops, causing a change in C_p , which for flexible molecules usually is a decrease. When measured by the heat capacity at a specified cooling rate, the glass transition is defined at the point of half-vitrification. Such an experiment is shown in Figure 6.

As listed in Figure 1, the change in C_p at T_g is similar for flexible molecules when they are approximated as strings of beads. The dependence of T_g on the time-scale of the operation and its irreversible nature is by now well understood, although a definitive theory with a simple mathematical description has yet to be found.^{1,23} For a full discussion of the glass transition, it is necessary to consider all seven listed parameters and to remember its kinetic origin. For example, the glass-transition range from T_1 to T_2 may be as little as 5–10 K for homopolymers, but it increases as much as 10-fold or more in phases with interfaces across which stress is transferred, as by the partially decoupled tie molecules. The change in T_g by a change in the frequency of measurement by 1 decade is similarly 5–10 K, increasing with increasing frequency. This would lower T_g measured in the timescale of 1 h by 30–60 K when we wait 1 century. The question to be addressed now is whether this definition can be expanded to all solids, as implied by the boxed text in Figure 6.

In a heating experiment with crystalline materials, one is tempted to separate the solid state from the liquid state by the melting transition. A melting transition is usually treated as an equilibrium, first-order transition,²⁴ which is characterized by a change in the slope of G ; that is, it

shows a change in the entropy in the macroscopic, thermodynamic description, and microscopically, there is an increase in disorder. The change in the slope of G at the equilibrium transition temperature is equal to a latent heat divided by the temperature, with the latent heat being measurable by thermal analysis. Figure 7 displays a typical melting experiment by DSC. As in Figure 6, care must be taken that the common instrument lags of the DSC instrument are properly eliminated by calibration. For sharp-melting, one-component equilibrium crystals, the extrapolation of the peak temperature to the baseline of the solid heat capacity eliminates the instrument lag and gives a good measure of T_m . The marked peak area is the latent heat and must be obtained from the integral of the heat flow rate over a properly corrected baseline.¹

If the melting covers a broader temperature range (>1 K), the peak temperature (corrected for the instrument lag) is a measure for the temperature of the maximum rate of melting (at the given heating rate), and the equilibrium melting temperature is not available from the extrapolation to the baseline of the solid heat capacity but must be evaluated by separate experiments and, if needed, by extrapolation. In such cases of broad melting ranges, common for macromolecules, one can usually design the experiment such that the heating rate remains constant throughout the melting. Then, the curve in Figure 7 can be treated as an apparent heat capacity, which gives the latent heat on subtraction of the indicated baseline of the properly apportioned heat capacities of the solid and liquid. With care, the necessary extrapolations of the latent heat with the temperature and crystallinity to the equilibrium melting temperature still yield good approximations of the entropy changes. For full characterization of such a broad melting peak, all seven



The seven characteristic parameters of the melting transition

On ordering, the glass transition shifts to higher temperature, so that after crystallization, glass transition and melting can, but do not have to, occur simultaneously, i.e., for crystals T_m may be equal to T_g .

Figure 7 Schematic of the melting transition analyzed on heating and its defining parameters.¹ [Color figure can be viewed in the online issue, which is available at www.interscience.wiley.com.]

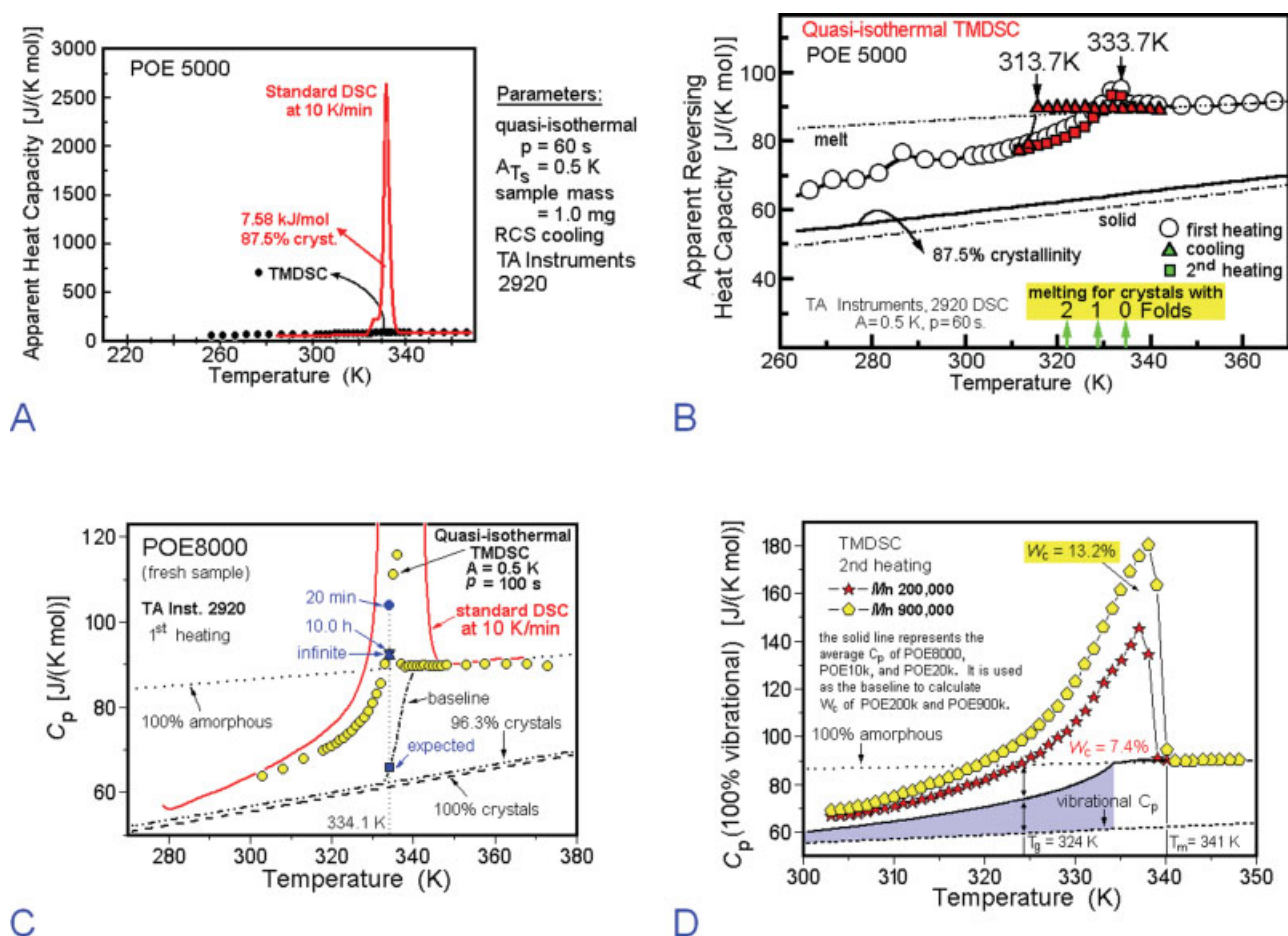


Figure 8 Melting of POE documenting a glass transition of the crystals below T_m .^{29,30} (A) standard DSC and quasi-isothermal TMDSC of extended-chain crystals of POE with a molar mass fraction of about 5000 Da; (B) enlargement of the TMDSC of the same sample shown in part A, illustrating a high C_p ; (C) the same sample shown in part B, but with an 8000-Da fraction and mainly a once folded morphology; and (D) separation of the thermodynamic C_p and reversible melting for high-molar-mass POE, showing the melting and glass transitions calculated for 100% crystallinity. The crystallinity of the 200,00- and 900,000-Da samples was 70 and 67%, respectively. [Color figure can be viewed in the online issue, which is available at www.interscience.wiley.com.]

characteristic parameters in Figure 7 should be specified, and for very broad melting ranges (>10 K), the changes in the involved functions of H and C_p with the temperature must be considered.

The ordering on cooling through first-order transitions is frequently connected to an increase in the packing fraction of the constituent molecules, which, in turn, can increase T_g . If this increase in T_g reaches T_m of the crystal, the disordering and transition to the solid state occur simultaneously, as was assumed in the drawing of Figure 7. In fact, this often observed case is at the root of the confusion of the definition of solids. Melting transitions may consist of both a disordering and a glass transition, and the kinetics of the glass transition is then determined by the melting rate. The heat capacity changes from the level of the C_p of the solid to that of the liquid, as is also shown in Figure 6 for a glass transition. The disordering transitions of mesophases usually change the heat capacities only a little, as can be seen in Figure 10(A,B) (shown later).

Their glass transition is at a much lower temperature than the disordering transition.

With modern TMDSC, the thermodynamic heat capacity can be separated from the latent heat effects. For nonequilibrium transitions, there is no response from the latent heat to the reversing temperature.²⁵ Any interfering slow changes in the crystalline order can be avoided with quasi-isothermal measurements in which the sample is modulated about a constant base temperature until it has reached a steady state or equilibrium.²⁶ Any remaining reversible ordering transition also can be eliminated by an increase in the modulation frequency so that the phase transition contributes negligibly to the calorimeter response.²⁷ Many examples of such TMDSC experiments have been reviewed and have contributed to a better understanding of the overlapping of glass and ordering transitions.²⁸ Next, a number of sample thermal analyses will be reviewed to illustrate the importance of the separate discussion of glass and melting transitions.

EXAMPLES OF GLASS AND ORDERING TRANSITIONS

Poly(oxyethylene) (POE): example of a crystal with a glass transition

POE, summarized in Figure 8, is next to polyethylene the most studied linear macromolecule. Figure 8(A) illustrates the apparent heat capacity of a crystalline, low-molar-mass POE, which was determined by standard DSC and quasi-isothermal TMDSC.²⁹ At the chosen magnification, the melting of the POE crystals seems fully irreversible, as expected for macromolecules. The melting peak appears only in the standard DSC. The quasi-isothermal TMDSC shows only the response due to the heat capacity. In the quasi-isothermal TMDSC, the melting is observed during the initial raising of the base temperature when the experiment is started. Data are collected usually after 10 min of modulation. By then, all irreversible melting and possible recrystallization or annealing have ceased. The latent heat contribution to the apparent heat capacity of standard DSC, however, is rather large, so that a much expanded scale for TMDSC, as shown in Figure 8(B), is needed to see the change in C_p in the melting range. Surprisingly, the measured reversible heat capacity is larger than the calculated vibrational contribution, as evaluated for polyethylene in Figure 3. In fact, it approaches the level of the liquid before the major irreversible melting starts. This behavior appears to signal a broad glass transition.

A more detailed look was taken at a larger number of POE fractions and whole samples with molar masses up to 900,000 Da.³⁰ Figure 8(C) shows that at a molar mass of 8000, at which crystals are mainly folded sharply once but the crystallinity is still very high, the reversing latent heat is small and mainly due to a slow reorganization to better crystals. After more than 10 h of quasi-isothermal experimentation, the reversible C_p is close to that of the liquid. This high heat capacity is much more than expected from the crystal already melted, as indicated by the calculated vibrational baseline marked in the figure. Even the defect contributions in the crystals, as seen for the equally mobile polyethylene in Figure 5, are not able to explain the liquid-like C_p before significant melting.

At a higher molar mass, POE changes to a typical semicrystalline polymer and shows increasing small amounts of reversible melting, as seen for many macromolecules.²⁸ Figure 8(D) displays the apparent, reversible C_p after correction to 100% crystallinity.³⁰ Clearly there is a T_g at 324 K, preceding the end of melting by almost 20 K. Separate X-ray data on the same samples indicated no change in the crystal structure before melting and no significant change in the size of the coherently scattering crystal domains but a distinct break in the expansivity of the unit cell volume at the glass transition,³¹ as is normally seen in

the expansivity from a solid to a liquid.¹ This behavior is that of a glass transition of a crystal. Additional glass-transition-like behavior of POE crystals is the change of its T_g with the molar mass, as seen from a comparison of Figure 8(D) and Figure 8(B), in which the T_g of POE5000 seems to be 270 K. This compares with the T_g of fully amorphous POE of 206 K.⁷

Effect of crystals on the glass transition of neighboring noncrystalline phases

Because even within the confines of a crystal it may be possible to show a glass transition, the coupling between crystals and the surrounding phases in semicrystalline polymers needs to be investigated. In particular, because the amorphous and crystalline phases approach nanophase sizes, their properties are expected to change from the bulk properties.¹ Figure 9(A) illustrates the calorimetry of the phase transitions in melt-crystallized poly(butylene terephthalate) (PBT).³² The initial glass transition at 314 K covers only 42.4% of the sample. With a crystallinity of 36.3%, this leaves 21.3% of the noncrystalline material unaccounted for. This part of the sample is considered a rigid-amorphous fraction (RAF)³³ and has been linked to the stress transmitted across the crystal-to-amorphous interface. From the analysis of the thermodynamic C_p calculated as in Figure 2 for polyethylene, one can judge the glass transition of the RAF to occur between 360 and 400 K at a T_g of 375 K. The typical equation for the evaluation of C_p from crystallinity, and vice versa, is listed in the figure and can naturally only be used down to 400 K, the upper limit of the T_g of the RAF. In accord with this interpretation, a more precise latent heat can be calculated from the DSC trace, and the reversing melting can be calculated from the quasi-isothermal TMDSC. Below 360 K, the thermal characterization requires us to consider the RAF as a second solid phase that is present in addition to the crystals. Its higher glass transition justifies this identification as a new nanophase.⁴ Below about 300 K, the mobile-amorphous phase also is solid.

This three-phase structure is also expected to apply to quenched samples of PBT of only about 10% crystallinity, as shown in Figure 9(B) and its insert. In this sample, irreversible cold crystallization on heating starts in the glass-transition region of the mobile-amorphous fraction, and the glass transition of the RAF produced on cold crystallization overlaps the beginning of melting. This sample can be analyzed only with the apparent heat capacity, as measured by DSC and TMDSC and written at the top of Figure 9(B) with separate input about the changes in the C_p of the two amorphous phases in their glass-transition regions. The analysis in the presence of RAF is a major complication from the simpler case illustrated in Figure 7.

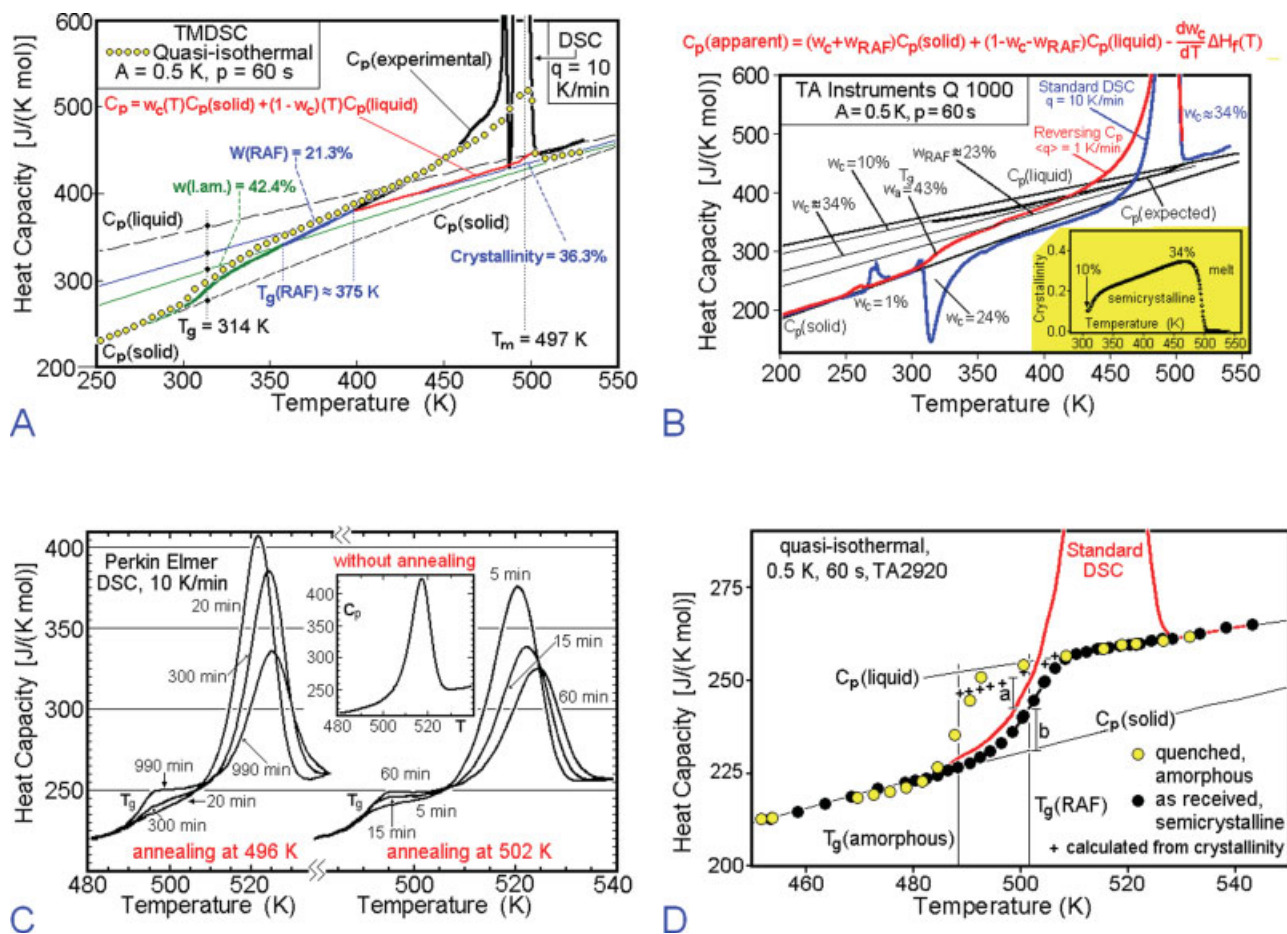


Figure 9 Analysis by DSC and TMDSC of the transitions in (A,B) PBT, with a glass transition of the RAF below the melting transition,³² and (B) PPO, with a glass transition of the RAF above the melting transition.^{36,37} [Color figure can be viewed in the online issue, which is available at www.interscience.wiley.com.]

Only with an understanding of the solid and liquid states with their structure and the molecular motion is one able to design optimum materials.

Although PBT is an example for a semicrystalline material with a T_g of the RAF below T_m , polyethylene is an example that shows only a broadening of the glass transition of the mobile–amorphous fraction and no separate transition of a rigid–amorphous phase. Although calorimetry cannot identify a separate third phase with a distinct glass transition, electron microscopy could identify an interface between the crystalline and amorphous phases with limited mobility,³⁴ as one would expect because of the stress transfer across the crystal surface. Also, an analysis of the highly stretched, gel-spun polyethylene fibers shows a mobile crystalline phase with a contribution to the latent heat on melting of the overall structure, but it also contributes prominently to the broadened glass transition.³⁵

In Figure 9(C,D), the behavior of poly(oxy-2,6-dimethyl-1,4-phenylene) (PPO) is presented. In this case of stiffer polymer chains, T_g of the RAF is moved

beyond T_m . The center graph of Figure 8(C) illustrates that there is no glass transition at all below the melting peak of an approximately 30% crystalline PPO.³⁶ On annealing below T_m , however, the sample develops a glass transition but also reduces its crystallinity, as seen in the two sets of annealing experiments, one at 496 K and the other at 502 K, both below the major melting peak in the center. The solution of this riddle of how melting could occur below T_m is given in Figure 9(D), in which TMDSC is added to the analysis.³⁷ At first, there is no reversible melting in the semicrystalline polymer (filled circles). Second, the quenched amorphous polymer has a lower T_g than the observed T_m . Third, the quasi-isothermal data of the semicrystalline PPO show a T_g that is also below the T_m seen with standard DSC but, upon the measurement of the crystallinity, decreases in parallel with an increase in the melted PPO. This means that the melting is governed by the kinetics of the glass transition of the RAF. The glassy RAF phase hinders the melting of the crystals until it reaches enough mobility for the given timescale of the experiment. Without being coupled to

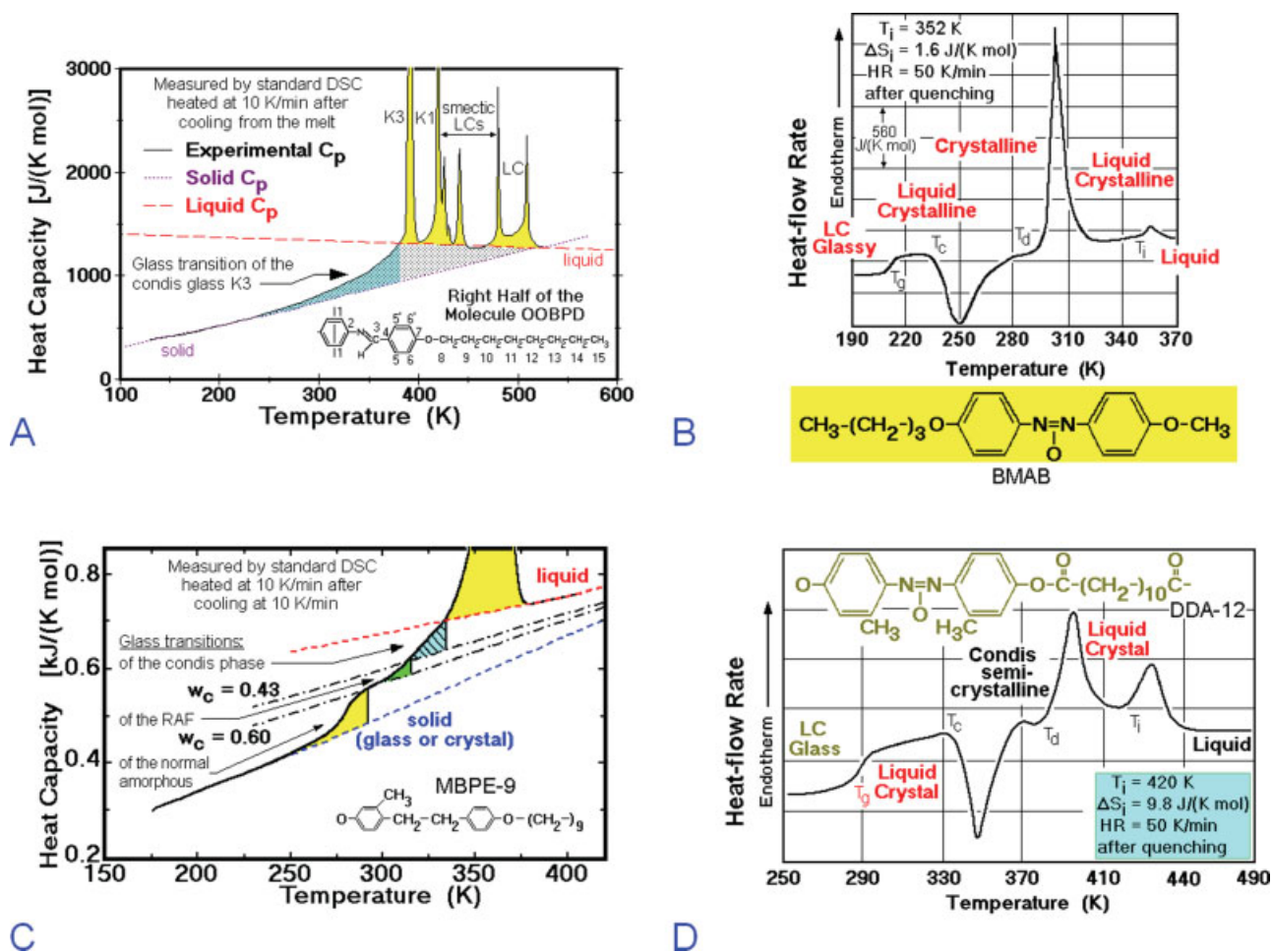


Figure 10 Standard DSC of mesophase samples: (A) the transitions of the LCs and condis crystals of OOBPD³⁸ (the vibrational heat capacity of the solid is reached only below the glass transition of the condis crystal; note also the change in the order outside the transition peaks in the nematic LC phase); (B) the transitions of BMAB, a small molecule LC with an ordering transition;³⁹ (C) the three glass transitions of MBPE-9;⁴⁰ and (D) the thermal analysis of liquid-crystalline DDA-12 with partial condiss crystallinity.⁴¹ [Color figure can be viewed in the online issue, which is available at www.interscience.wiley.com.]

the enclosing, glassy RAF, the PPO crystals would melt below 500 K at a much faster rate and probably also show some reversible melting. This example shows that it is possible to change not only the kinetics of the glass transition on crystallization or melting but also the kinetics of melting on devitrification of the glass. All these observations can now be easily explained by the realization of the interplay between glass and melting transitions.

Glass transitions of mesophases

The separations of ordering and glass transitions, which has been discovered only recently for crystals, is common for mesophases.⁵ On cooling from the liquid, one finds one or more first-order transitions that produce increasing perfection of the molecular packing. The large-amplitude motion, characteristic for the

mesophases, freezes at a separate glass transition at a lower temperature whenever further ordering to a crystal is not possible or sufficiently slow. Figure 10(A) illustrates the transitions in the small molecule *N,N'*-bis(4-*n*-octyloxybenzal)-1,4-phenylenediamine (OOBPD).³⁸ On cooling, at first, a nematic LC appears. This ordering transition is fully reversible when studied by TMDSC. The structure of the nematic phase has only a minor amount of one-dimensional, orientational order, allowing almost free translational, liquid-like motion. On further cooling, several smectic LCs with some two-dimensional order result before the K1–K3 phases are formed. The K phases were originally thought to be crystalline, but it was more recently proven that in these phases many of the paraffinic C–C bonds are free to undergo conformational, large-amplitude motion; that is, they are condiss crystals.⁶ After the formation of K3, sufficient large-amplitude motion is still possible to yield a C_p that is

close to that of the liquid. Only further lowering of the temperature results in a solid CD glass, as indicated in Figure 10(A). The appearance of the glass transition is quite similar to that of POE in Figure 8(D).

Figure 10(B) illustrates the glass transition of another LC-forming small molecule, *p*-butyl-*p*'-methoxyazoxybenzene (BMAB).³⁹ This LC can be quenched to a liquid-crystalline, solid glass (see the LC glass in Fig. 1). Its crystallization is sufficiently slow that on quenching only about 20% of the crystals grow before LC glass formation stops the large-amplitude molecular motion necessary for crystallization. On heating, the glass transition produces the metastable, supercooled LC at T_g . On further heating, the liquid-crystalline phase becomes unstable and cold-crystallizes at the crystallization temperature (T_c) to a crystalline solid, which then, at the disordering transition temperature (T_d), changes to the stable liquid-crystalline phase, which has a final disordering transition to the isotropic liquid at the isotropization temperature (T_i). Note that the three close-to-liquid phases at about 220, 340, and 370 K have a higher linear heat-flow-rate baseline than the two solid phases at 190 and 280 K. Also, the crystallization and melting peaks are much larger than the isotropization peak, as expected from the small amount of order present in an LC.

The next two examples are of linear, flexible macromolecules. Figure 10(C) presents the DSC analysis of condis crystals of poly[oxy(3-methyl-1,4-phenylene)ethylene-1,4-phenyleneoxynonamethylene] (MBPE-9),⁴⁰ which is to be compared with the small molecule OOBPD in Figure 10(A). Below the order-disorder transition of the condis crystalline phase, it has a transition range showing overlapping glass transitions for 43% condis crystals, 17% rigid-amorphous phase, and 40% mobile-amorphous phase. In Figure 10(D), liquid-crystalline poly(oxy-2,2'-dimethylazoxybenzene-4,4'-dioxidodecanoyl) (DDA-12)⁴¹ illustrates a behavior similar to that of the small molecule BMAB. The only difference is the lower heat of ordering and disordering, which is the result of only partial crystallinity in the semicrystalline polymer. The entropy of isotropization of the polymer, in turn, is larger for the polymeric LC, suggesting the effect of the need to parallelize the continuing polymer chains.

CONCLUSIONS

A review of the macroscopic, thermodynamic descriptions of all types of phases is given in Figure 1, including equilibrium and nonequilibrium phases. At the top, the figure summarizes five phases that are solids of increasing degrees of order from the amorphous glass to the crystal. The next four phases are increasingly liquid and also increasingly more disordered. Finally, the bottom phase is a dilute phase, a gas. A complete description of these phases and their dif-

ferent properties must make use of the molecular structure and motion. The link of the microscopic description to the thermodynamics is given by the entropy, which specifies the degree of disorder, and the heat capacity, which is governed by the molecular motion. Although in the solid state vibrational motion is dominant, the increasing liquidity is caused by cooperative, large-amplitude motions seen as translation, rotation, and conformational, internal rotation. Their connection to the heat capacity is illustrated in Figures 2–5. The types of thermal transition between the phases, which may be in equilibrium or arrested on cooling, are shown in Figures 6 and 7. The more subtle glass transition is linked to the freezing and unfreezing of the cooperative large-amplitude motion and can be used in an operational definition of the solid state. The first-order transitions, which are often closer to equilibrium, are linked to ordering and disordering and can be used to determine the entropy either directly or by extrapolation. Figures 8–10 illustrate the interrelationships between the two types of transitions. The glass transition can occur independently and links then phases of identical entropy (order), it can overlap or occur simultaneously with first-order transitions, and it can also be influenced by interactions across the phase boundaries. In all cases, the glass transition is the key to identify the solid below T_g . The prior assumption that the much more conspicuous crystal-to-melt, first-order transition also defines the solid state is not a tenable operational definition. Only if a glass transition occurs simultaneously with the first-order transition is it also a solid-liquid transition.

The ATHAS effort is supported by the Polymers Program of the Materials Division of the National Science Foundation (grant DMR-0312233) and by the Division of Materials Sciences and Engineering, Office of Basic Energy Sciences, U.S. Department of Energy at Oak Ridge National Laboratory, which is managed and operated by UT-Battelle, LLC, for the U.S. Department of Energy under contract number DOE-AC05-00OR22725.

References

1. (a) Wunderlich, B. *Thermal Analysis of Polymeric Materials*; Springer: Berlin, 2005. See also (b) *Thermal Analysis of Materials*, 2007 (a 36-lecture computer course available via downloading through the internet at <http://athas.prz.rzeszow.pl>; <http://www.scite.eu> or via the European Virtual Institute for Thermal Metrology at <http://www.evitherm.org/index.asp> at the home page for thermal analysis and calorimetry) and (c) *Macromolecular Physics*; Academic: New York, 1973, 1976, and 1980; Vols. 1–3 [which is available as a pdf reprint with a new preface and electronically searchable index, also from <http://www.scite.eu>].
2. Prigogine, I. *Introduction to Thermodynamics of Irreversible Processes*, 3rd ed.; Interscience: New York, 1967.
3. Wunderlich, B. *Thermochim Acta* 2000, 355, 43.
4. Chen, W.; Wunderlich, B. *Macromol Chem Phys* 1999, 200, 283.

5. Wunderlich, B.; Grebowicz, J. *Adv Polym Sci* 1984, 60, 1.
6. Wunderlich, B.; Möller, M.; Grebowicz, J.; Baur, H. *Conformational Motion and Disorder in Low and High Molecular Mass Crystals*; *Advances in Polymer Science* 87; Springer: Berlin, 1988.
7. Advanced Thermal Analysis Data Bank described in (a) Wunderlich, B. *Pure Applied Chem* 1995, 67, 1019; (b) *Handbook of Thermal Analysis and Calorimetry*; Cheng, S. Z. D., Ed.; Elsevier: Amsterdam, 2002; Vol. III, p 1. For a collection of critically analyzed data, see the 2006 ATHAS website at: (c) <http://athas.prz.rzesow.pl>.
8. Baur, H. *Thermophysics of Polymers*; Springer: Berlin, 1999.
9. Barnes, J.; Fanconi, B. *J Phys Chem Ref Data* 1978, 7, 1309.
10. Debye, P. *Ann Phys* 1912, 39, 789.
11. Tarasov, V. V. *Zh Fiz Khim* 1950, 24, 111.
12. Wunderlich, B.; Baur, H. *Fortschr Hochpolym Forsch* 1970, 7, 151.
13. Einstein, A. *Ann Phys* 1907, 22, 180 (a correction is shown on p 800).
14. Pyda, M.; Wunderlich, B. *J Polym Sci Part B: Polym Phys* 2002, 40, 1245.
15. Kauzmann, W. *Chem Rev* 1948, 43, 219.
16. Sumpter, B. G.; Noid, D. W.; Liang, G. L.; Wunderlich, B. *Adv Polym Sci* 1994, 116, 27.
17. Kim, Y.; Strauss, H. L.; Snyder, R. G. *J Phys Chem* 1989, 93, 7520.
18. Wunderlich, B.; Pyda, M.; Pak, J.; Androsch, R. *Thermochim Acta* 2001, 377, 9.
19. Merriam Webster's Collegiate Dictionary, 11th ed.; Merriam-Webster: Springfield, MA, 2003 (see also <http://www.m-w.com>).
20. Bridgman, P. W. *The Logic of Modern Physics*; Arno: New York, 1980.
21. Staveland, L. A. K. *Annu Rev Phys Chem* 1962, 13, 351.
22. Starkweather, H. W., Jr. *J Polym Sci Polym Phys Ed* 1979, 17, 73.
23. *Assignment of Glass Transition Temperatures Using Thermo-mechanical Analysis*; Seyler, R. J., Ed.; ASTM STP 1249; American Society for Testing and Materials: Philadelphia, PA, 1994.
24. Ehrenfest, P. *Proc Acad Sci Amsterdam* 1993, 36(Suppl. 75b), 153.
25. Reading, M.; Elliott, D.; Hill, V. *Proc NATAS Conf* 1992, 21, 145.
26. Wunderlich, B.; Jin, Y.; Boller, A. *Thermochim Acta* 1994, 238, 277.
27. Merzlyakov, M.; Wurm, A.; Zorzut, M.; Schick, C. *J Macromol Sci Phys* 1999, 38, 1045.
28. Wunderlich, B. *Prog Polym Sci* 2003, 28, 383.
29. Ishikiriyama, K.; Wunderlich, B. *Macromolecules* 1997, 30, 4126.
30. Qiu, W.; Pyda, M.; Nowak-Pyda, E.; Habenschuss, A.; Wunderlich, B. *Macromolecules* 2005, 38, 8454.
31. Qiu, W.; Pyda, M.; Nowak-Pyda, E.; Habenschuss, A.; Wunderlich, B. *J Polym Sci Part B: Polym Phys* 2007, 45, to appear.
32. Pyda, M.; Nowak-Pyda, E.; Heeg, J.; Huth, H.; Minakov, A. A.; Di Lorenzo, M. L.; Schick, C.; Wunderlich, B. *J Polym Sci Part B: Polym Phys* 2006, 44, 1364.
33. Suzuki, H.; Grebowicz, J.; Wunderlich, B. *Br Polym J* 1985, 17, 1.
34. (a) Kunz, M.; Möller, M.; Heinrich, U.-R.; Cantow, H.-J. *Makromol Chem Symp* 1988, 20, 147; (b) Kunz, M.; Möller, M.; Heinrich, U.-R.; Cantow, H.-J. *Makromol Chem Symp* 1989, 23, 57.
35. Kwon, Y. K.; Boller, A.; Pyda, M.; Wunderlich, B. *Polymer* 2000, 41, 6237.
36. Cheng, S. Z. D.; Wunderlich, B. *Macromolecules* 1987, 20, 1630.
37. Pak, J.; Pyda, M.; Wunderlich, B. *Macromolecules* 2003, 36, 495.
38. Cheng, J.; Jin, Y.; Liang, G.; Wunderlich, B.; Wiedemann, H. G. *Mol Cryst Liq Cryst* 1992, 213, 237.
39. Grebowicz, J.; Wunderlich, B. *J Mol Cryst Liq Cryst* 1981, 76, 287.
40. Jin, Y.; Cheng, J.; Wunderlich, B.; Cheng, S. Z. D.; Yandrasits, M. A. *Polym Adv Technol* 1994, 5, 785.
41. Grebowicz, J.; Wunderlich, B. *J Polym Sci Polym Phys Ed* 1983, 21, 141.